Journal of the Serbian Chemical Society
JSCS-info@shd.org.rs • www.shd.org.rs/JSCS

*J. Serb. Chem. Soc. 78* (12) 1993–2005 (2013)
*JSCS–4546*

UDC 546.96+546.93+544.478+
621.352:539.196:541.574
*Original scientific paper*

# XPS and STEM study of the interface formation between ultra-thin Ru and Ir OER catalyst layers and Perylene Red support whiskers•

LJILJANA L. ATANASOSKA[1]*, DAVID A. CULLEN[2] and RADOSLAV T. ATANASOSKI[1]*

*[1]3M Co., 3M Center, St. Paul, MN, 55144-1000 USA and [2]Materials Science and Technology Division, Oak Ridge National Laboratory, Oak Ridge TN 37831 USA*

(Received 27 September 2013)

*Abstract*: The interface formation between nano-structured Perylene Red (PR) whiskers and the oxygen evolution reaction (OER) catalysts ruthenium and iridium was studied systematically by XPS and STEM. The OER catalyst over-layers with thicknesses ranging from ≈0.1 to ≈50 nm were vapor deposited onto PR *ex situ*. STEM images demonstrated that, with increasing thickness, Ru and Ir transform from amorphous clusters to crystalline nanoparticles, which agglomerate with increased over-layer thickness. XPS data showed a strong interaction between Ru and PR. Ir also interacts with PR although not to the extent seen for Ru. At low coverages, the entire Ru deposit was in the reacted state while a small portion of the deposited Ir remained metallic. Ru and Ir bonding occur at the PR carbonyl sites as evidenced by the attenuation of carbonyl photoemission and the emergence of new peak assigned to C–O single bonds. Curve fitting analysis and the derived stoichiometry indicated the formation of metallo–organic bonds. The co-existence of oxide bonds was also apparent.

*Keywords:* fuel cell; catalyst; surface properties; deposition.

## INTRODUCTION

Highly active oxygen evolution reaction (OER) catalysts based on deposited Ru and Ir onto Pt-coated nano-structured Perylene Red whiskers (3M Pt–NSTF) are currently being investigated for polymer electrolyte membrane fuel cell (PEMFC) applications. A key issue for the successful transition of PEMFC technology from the development to the pre-commercial phase is failure of the catal-

* Corresponding author. E-mail: rtatanasoski@mmm.com

• To Prof. Branislav Nikolić, our long time friend and colleague, for his many contributions in the area of fundamental and applied electrochemistry.

doi: 10.2298/JSC130927111A

yst and the other thermodynamically unstable membrane electrode assembly (MEA) components during the so-called transient conditions, start-up/shutdown (SU/SD) and cell reversal (CR). If left unchecked, during these periods, the electrodes can attain potentials of up to 2 V,[1–3] leading to rapid carbon corrosion and Pt dissolution. To improve the durability of the fuel cell catalyst and support, minute loadings of Ru/Ir OER catalysts (2 and 10 μg $cm^{-2}$) were incorporated into the electrode to favor water electrolysis over carbon corrosion. This has resulted in vastly improved fuel cell robustness and durability during transient conditions due to a reduction in the peak cell voltages.[1,2]

During the course of a study of OER catalysts sputter-coated on Pt–NSTF, it was discovered that the Ru/Ir catalyst had unusually high activity and stability when grown on Pt–NSTF.[4,5] Furthermore, a distinct difference in the C 1s–Ru 3d line shape between 2 and 10 μg $cm^{-2}$ OER catalyst loadings was observed, despite the fact that the OER catalysts were sputter-coated over a relatively thick Pt film. The reacted Ru $3d_{5/2}$ shoulder, shifted to a higher binding energy (BE) with respect to the BE location of the un-reacted Ru $3d_{5/2}$ peak, which was more pronounced for the 2 μg $cm^{-2}$ loading than for the 10 μg $cm^{-2}$ loading. Curve fitting analysis and the obtained O, C and Ru stoichiometry balance suggested a chemical interaction of Ru with the underlying Perylene Red support and the formation of organo–metallic type bonds, such as $Ru(OC)_x$ or $Ru(CO)_x$. The STEM images confirmed the existence of discontinuities in the Pt coating, indicating of the availability of exposed bare Perylene Red sites for interaction with Ru.

In order to confirm that the existence and the anchoring action of Ru–O–C bonds at the interface with Perylene Red (PR) was potentially the cause of the Ru-containing OER catalyst stability, a systematic study of the interfaces between Ru, Ir and PR was conducted. The Ru and Ir over-layers with thicknesses ranging from 0.2 to 48 nm and 0.1 to 34.8 nm, respectively, were formed onto PR whiskers *ex situ* by physical vapor deposition. Scanning transmission electron microscopy (STEM) was used to study the growth of Ru and Ir on the Perylene Red support. The XPS core level spectra and curve fitting analysis revealed a strong interaction between Ru and PR. Ir was also found to interact with PR although not to the extent seen for Ru. At low coverages, the entire Ru deposit was in the reacted state, while a small portion (≈10 at. %) of the deposited Ir remains metallic. Ru and Ir bonding occurred at the PR carbonyl sites, as evidenced by the preferential attenuation of carbonyl carbon photoemission and the emergence of new carbon peak assigned to C–O single bonds. Curve fitting analysis and the derived stoichiometry indicated the formation of $Ru(OC)_x$ or $Ru(CO)_x$ metallo–organic bonds. The co-existence of oxide bonds was also apparent.

## EXPERIMENTAL

### *Materials and sample preparation*

Ru and Ir over-layers were deposited on a Perylene Red whiskers (3M NSTF) substrate by a DC-magnetron sputtering process. A Mills-Lane vacuum deposition system was equipped with 4 CTI cryo-pumps, a Pfeiffer 450 turbo-pump and specially designed sputtering target assemblies from the Sierra Applied Science Company. High purity Ru and Ir (99.99+ %) from Sophisticated Alloys (Butler, PA) were used for the sputtering targets. Ultra high purity Ar was used as the sputtering gas with magnetron power range from 30–300 Watts. A pre-sputter of each target was performed to clean the surface. Before deposition, the PVD chamber was evacuated to a base pressure of $7\times10^{-7}$ Torr.

### *XPS Surface analysis*

Chemical states and elemental compositions of the OER catalyst over-layers on Perylene Red NSTF were analyzed by X-ray photoelectron spectroscopy, using a Kratos Axis Ultra™ XPS system at a base pressure below $10^{-9}$ Torr. The monochromatic AlK$\alpha$ (1486.6 eV) X-ray source was operated at 140 W (14 kV, 10 mA). A hemispherical electron energy analyzer was operated at constant pass energy of 160 eV for survey and 20 eV for the high-resolution spectra. The binding energy (BE) scale was calibrated relative to the BE of the C 1s peak. The spectra were acquired at a 90° take-off angle with respect to the sample surface. The data processing was realized with PHI MultiPak V8.2B, 2006 and Casa XPS V 2.3.16 Dev41 software. The curve fitting analysis of the core level spectra was based on summed Gaussian/Lorentzian GL functions, with a PHI line-shape to represent the asymmetric nature of the peaks and Shirley-type background subtraction. The Ru $3d_{5/2}$–Ru $3d_{3/2}$ spin orbital doublet branching ratio was constrained to 3:2 and their binding energy separation to 4.17 eV. The branching ratio and BE splitting of the Ir $4f_{7/2}$–Ir $4f_{5/2}$ spin orbital doublet were constrained for the fitting at their theoretical values 4:3 and 2.98 eV, respectively. The FWHM of resolved peaks was not constrained but was kept consistent with the allowed variations of ≈15 %.

### *STEM Characterization*

As-received OER catalyst-coated whiskers were prepared for STEM analysis by sonicating the material in methanol, then placing a small amount of the solution onto lacy carbon films supported on standard Cu-mesh TEM grids. A JEOL 2200FS probe-corrected STEM was used for complementary high-angle annular dark-field (HAADF).

## RESULTS AND DISCUSSION

### *XPS and STEM characterization of the evolving ruthenium–Perylene Red interface*

The C 1s core level spectra of the bare PR substrate (0 nm Ru thickness) and the C 1s–Ru 3d core level photoemission for Ru deposits from 0.2 to 48 nm are plotted together in Fig. 1. The bare PR C 1s core level spectra consisted of two distinct peaks, the main, more intense peak at ≈285 eV from the PR aliphatic and aromatic carbons and the less intense peak at ≈288 eV from the PR carbonyl carbon. The intensity ratio of the two PR carbon peaks is in agreement with the chemical structure.[6] The C 1s–Ru 3d core level spectra for Ru deposits are more complex because the PR aliphatic and aromatic carbon peak overlap with the Ru $3d_{3/2}$ photoemission. However, in spite of the complexity of the C 1s–Ru 3d line-

shape, its change with increasing Ru coverage clearly demonstrated that chemical interaction occurred at the Ru–PR interface. At the ultra low Ru coverages of 0.2 and 0.4 nm, a notable broadening of the Ru $3d_{5/2}$ peak and a visible BE shift of ≈2 eV, with respect to the metallic Ru $3d_{5/2}$ BE observed for the higher coverages of 12 and 48 nm, suggested the formation of multiple Ru oxidation states.[7] Moreover, the preferential attenuation of the PR carbonyl carbon peak and the emergence of a new carbon peak at 287 eV, associated with ether like C–O single bonds, indicated that the Ru chemical attack occurred preferentially at the PR carbonyl group sites.

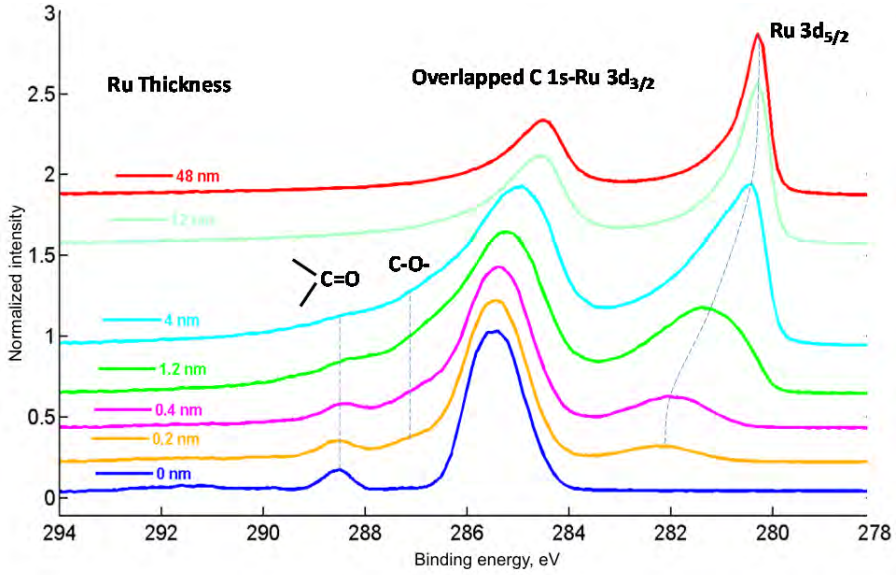


Fig. 1. C 1s core level spectra for bare PR substrate and C 1s–Ru 3d core level photoemission for Ru deposits from 0.2 to 48 nm in thickness.

The O 1s core level spectra of the evolving Ru–PR interface, shown in Fig. 2, further confirm the interaction at the interface. The Ru deposition on PR resulted in a striking increase in the intensity of the oxygen peak associated with ether like O–C bonds. In addition, with further ruthenium deposition, the appearance of an oxide oxygen peak was obvious.

Curve fitting analysis was realized in order to resolve the multiple Ru oxidation states and to quantify the chemical changes occurring at the growing interface. As seen in Fig. 3, from the curve fitting analysis example of C 1s–Ru 3d core level spectra for 1.2 nm Ru coverage, three different ruthenium chemical states were resolved. The resolved Ru $3d_{5/2}$ peaks I–III at a BE of ≈280.5, ≈281.5 and ≈282.5 eV came from un-reacted/metallic $Ru^0$, reacted $Ru^{x+}$ and reacted $Ru^{y+}$ states, respectively.

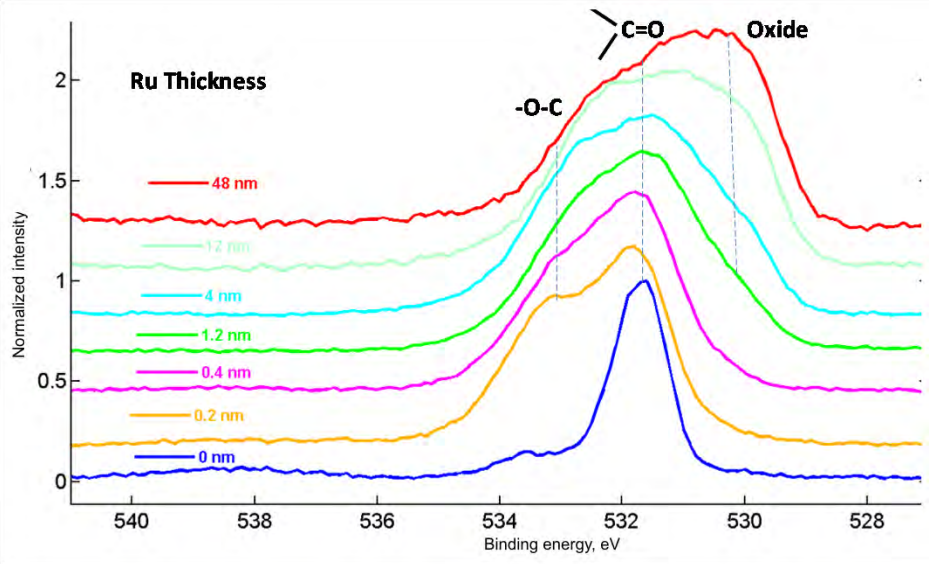


Fig. 2. O 1s core level spectra for bare PR substrate and O 1s core level photoemission for Ru deposits from 0.2 to 48 nm in thickness.

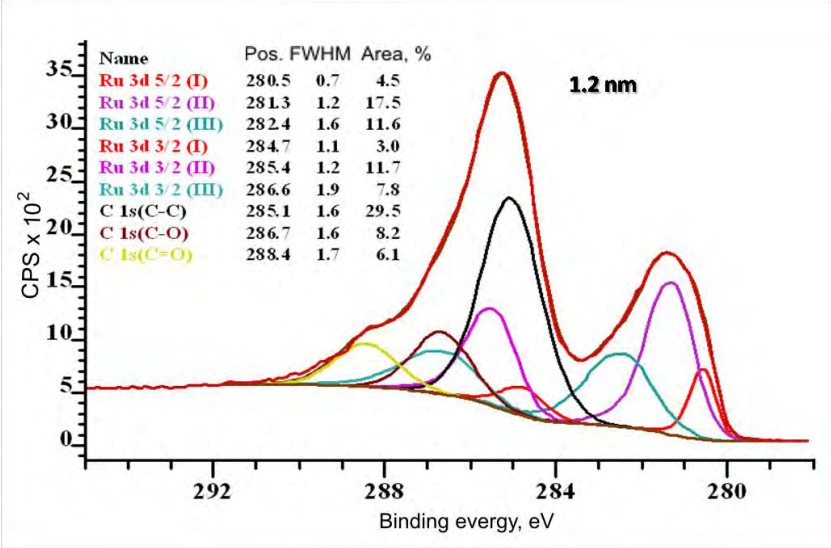


Fig. 3. Curve fitting analysis of the C 1s–Ru 3d core level spectra for 1.2 nm Ru coverage.

The results of C 1s–Ru 3d curve fitting analysis are plotted in Fig. 4 as a function of Ru deposit thickness. No un-reacted metallic Ru was present at the interface for ultra low Ru coverage, up to 1 nm. As expected, the increase in the contribution of metallic Ru resulted in an attenuation of the PR C–C photo-

emission. The attenuation behavior of the resolved $Ru^{x+}$ and $Ru^{y+}$ species suggested that organo–metallic Ru–O–C bonds contributed to their photoemission for Ru coverages up to 2–4 nm. Final state screening effects may also be involved in the photoemission of the resolved $Ru^{y+}$ species.[7] As seen from Fig. 4, there was an initial sharp increase in the contribution of both resolved Ru reacted states. Then, $Ru^{y+}$ species became attenuated by metallic Ru over-layers, while $Ru^{x+}$ remained flat due to its conversion into $RuO_x$ forms.

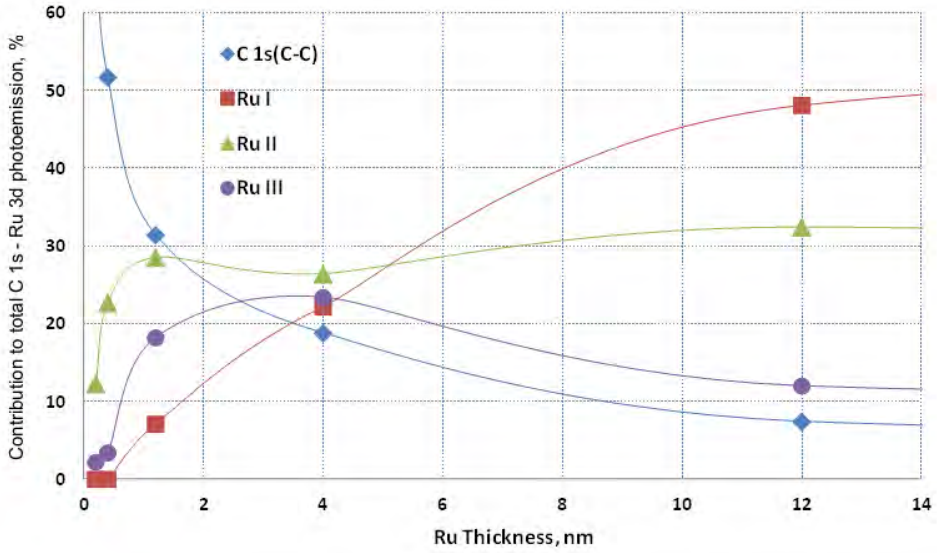


Fig. 4. Contribution of metallic and reacted Ru as a function of Ru thickness: Ru-I is unreacted/metallic $Ru^0$, Ru-II is reacted $Ru^{x+}$ and Ru-III is reacted $Ru^{y+}$.

The curve fitting analysis of both C 1s–Ru 3d and O 1s core level spectra along with the stoichiometry balance confirmed the chemical interaction of Ru with PR and formation of $Ru(OC)_x$ or $Ru(CO)_x$ metallo–organic bonds. The co-existence of oxide bonds was also apparent. The formation of Ru complexes with PR may result in multiple resonance hybrid states, such as those shown in Fig. 5. The metal–carbonyl group interaction is likely to occur and it was previously observed for molecules that have comparable structures to that of PR.[8,9]

High-angle annular dark-field (HAADF) STEM images of whiskers with Ru layer thicknesses of 0.2, 0.4, 1.2 and 4 nm are shown in Fig. 6. At the lowest loading, Ru was present in atomic clusters. As the loading increased, the Ru formed into crystalline nanoparticles, which further developed into an interconnected network. Even at 4.0 nm thickness, regions of bare PR were observed and mobile Ru atoms were visible in these exposed regions.

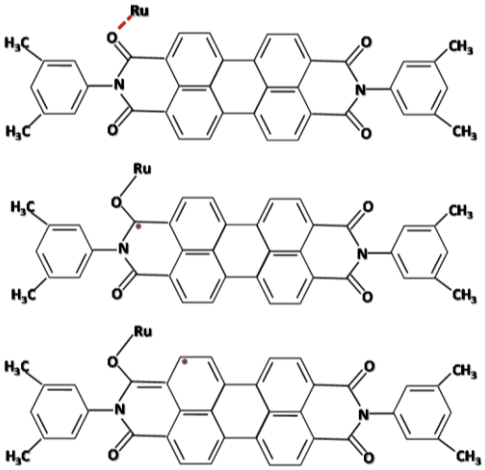


Fig. 5. Perylene Red–ruthenium interaction: Ru–O–C complex formation and possible resonance hybrid structures.

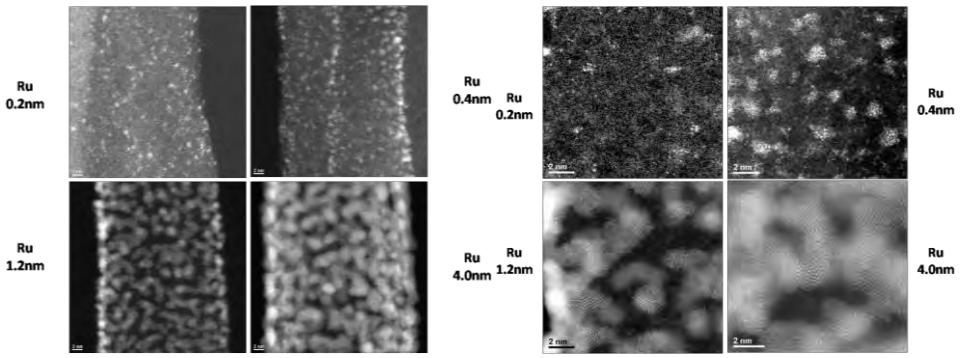


(a) (b)

Fig. 6. High-angle annular dark-field (HAADF) images of whiskers with Ru layers of thicknesses 0.2, 0.4, 1.2 and 4 nm taken at a) 4 M× and b) 10M× magnification.

*XPS and STEM characterization of an evolving iridium–Perylene Red interface*

The Ir 4f, C 1s and O 1s core level spectra in Figs. 7–9 demonstrate that interaction also occurred at the Ir–PR interface. At low Ir coverages, the Ir 4f peaks exhibit a line-shape broadening and a BE shift of ≈2 eV with respect to the BE location of metallic Ir. A preferential attenuation of the carbonyl carbon peak and the emergence of the ether carbon peak are also apparent from the C 1s core level spectra. The sharp increase in the oxygen peak associated with the ether oxygen bonds could also be seen from the O 1s core level spectra, although it was not so striking as in the case of Ru, which indicates a weaker interaction at the Ir–PR interface. The appearance of the oxide oxygen peak at higher Ir coverages also occurred at the Ir–PR interface.

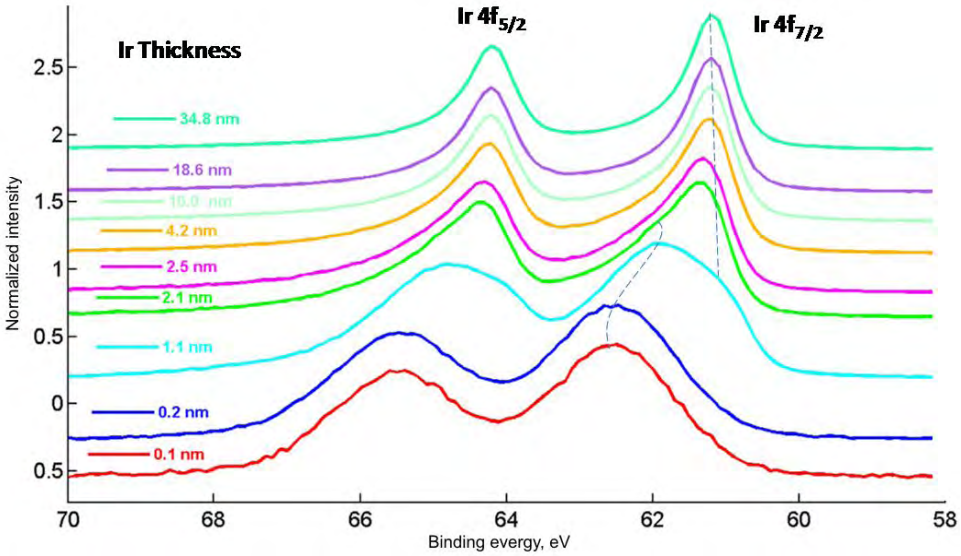


Fig. 7. Ir 4f core level photoemission for Ir deposits from 0.1 to 34.8 nm in thickness.

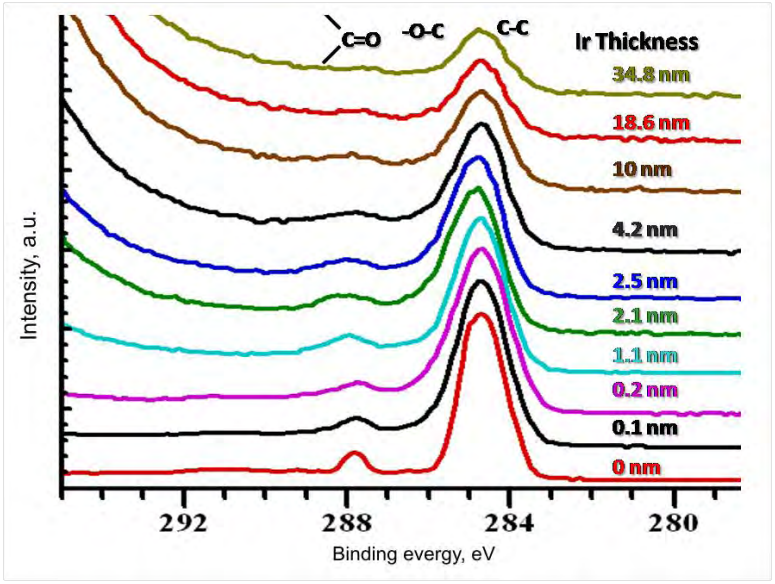


Fig. 8. C 1s core level photoemission for Ir deposits from 0.1 to 34.8 nm in thickness.

The curve fitting analysis of Ir 4f core level spectra resolved three different Ir chemical states. The Ir $4f_{7/2}$ peaks at BE of ≈ 61, ≈62 and 63 eV correspond to un-reacted/metallic Ir, reacted $Ir^{x+}$ and reacted $Ir^{y+}$ states, respectively.[8] The examples of curve fitting analysis of Ir 4f core level spectra realized for Ir thicknesses of 1.1 and 2.1 nm are presented in Fig. 10.

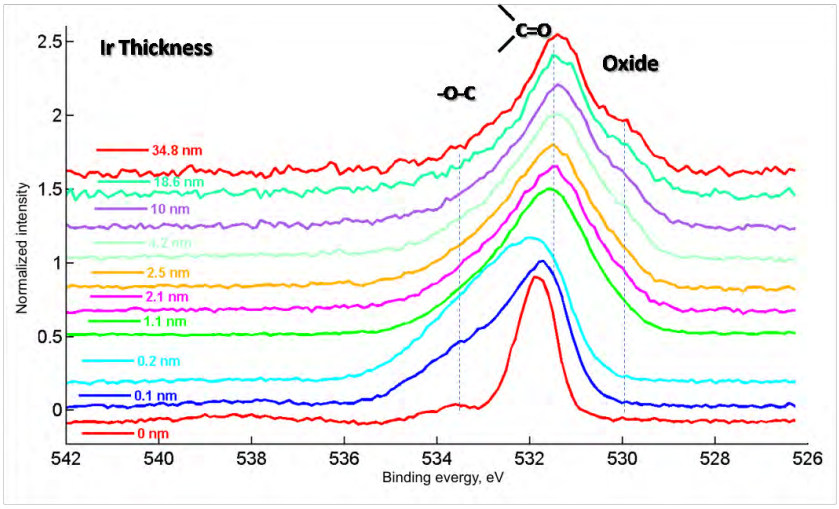


Fig. 9. O 1s core level photoemission for Ir deposits from 0.1 to 34.8 nm in thickness.

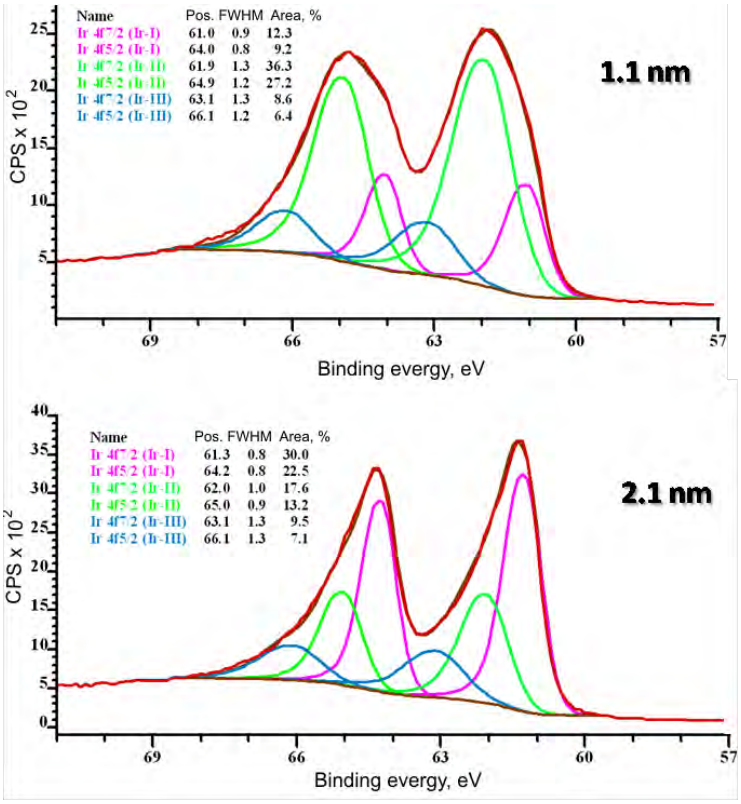


Fig. 10. Examples of Ir 4f core level curve fitting analysis realized for 1.1 and 2.2 nm thick Ir deposits on a PR substrate.

The results of Ir 4f curve fitting analysis are plotted in Fig. 11 as a function of the thickness of the Ir deposit. Fig. 11 shows that un-reacted metallic Ir was present at the interface for the lowest Ir coverages of 0.1 and 0.2 nm, which further confirmed the weaker interactions at the Ir/PR interface compared to those at the Ru–PR interface. The attenuation behavior of the resolved $Ir^{x+}$ and $Ir^{y+}$ species suggested that organo–metallic Ir–O–C bonds ($Ir^{y+}$) were formed only at the lowest Ir coverage of 0.1 nm and that they were immediately substantially attenuated by the growing contribution of Ir oxide bonds ($Ir^{x+}$). As in the case of Ru, final state screening effects may also participate in the photoemission of the resolved $Ir^{y+}$ species.[10] The attenuation of $IrO_x$ ($Ir^{x+}$) by the growing metallic Ir occurred sharply at ≈1 nm.

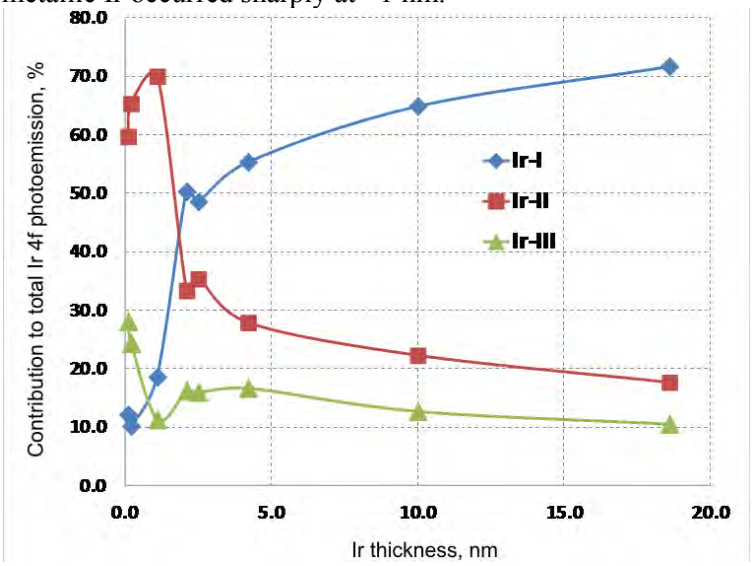


Fig. 11. Contribution of metallic and reacted Ir as a function of Ir thickness: Ir-I is un-reacted/metallic $Ir^0$, Ir-II is reacted $Ir^{x+}$ and Ir-III is reacted $Ir^{y+}$.

As in the case of the Ru–PR interface, the formation of organo–metallic iridium bonds along with the Ir oxide was confirmed by the curve fitting analysis of both Ir 4f and O 1s core level spectra along with the stoichiometry balance.

The contribution of resolved un-reacted and reacted species for both interfaces are plotted together in Fig. 12 to illustrate how much stronger the interaction of Ru with PR is relative to that of Ir with PR.

HAADF-STEM images of PR whiskers with Ru and Ir layer thicknesses of approximately 1.2 and 0.2 nm are compared in Fig. 13. The Ir layer appears to deposit in the same manner observed previously for Ru, with the initial formation of small clusters at the lowest loading followed by the formation of crystalline nanoparticles with increased deposition.

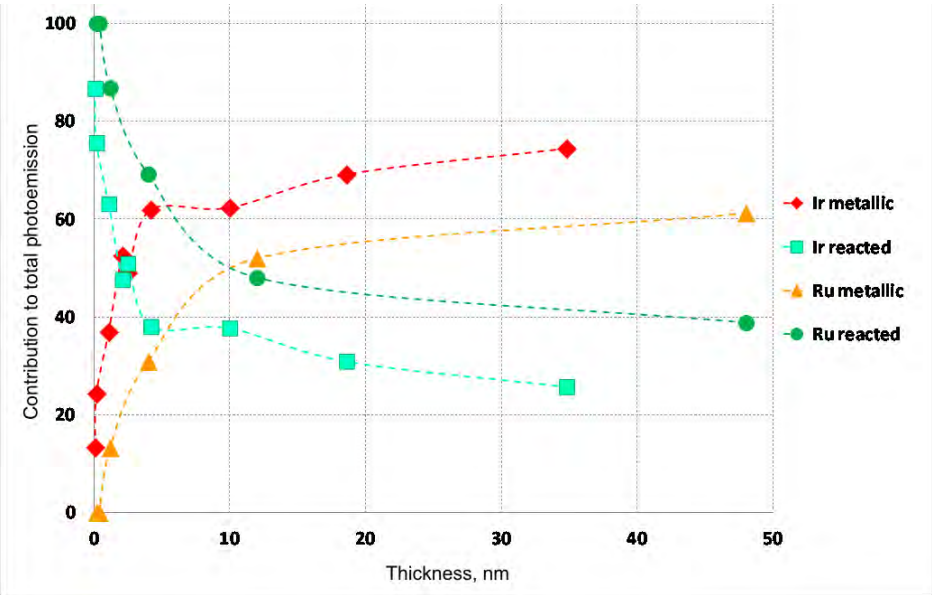


Fig. 12. Comparison of the evolving interface behavior of Ir and Ru with PR: Contribution of metallic and reacted states as a function of deposit thickness.

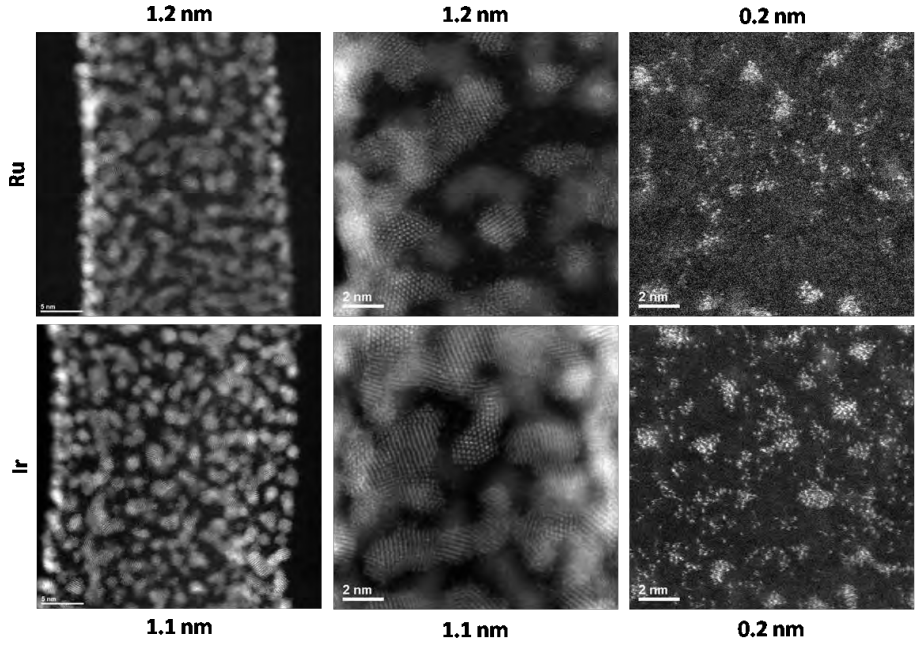


Fig. 13. Comparison of Ru–PR and Ir–PR interface nano-morphology for two different Ru and Ir thicknesses.

## CONCLUSIONS

A systematic study of evolving Ru–PR and Ir–PR interfaces was conducted. A strong interaction of ruthenium with Perylene Red whiskers was found to the extent that no metallic ruthenium was present at low Ru coverage. Curve fitting analysis and the stoichiometry balance confirmed the presence of metallo––organic bonds, such as $Ru(OC)_x$ and $Ru(CO)_x$. A co-existence of oxide bonds was also apparent. Interaction of iridium with Perylene Red whiskers was also found, although not to the extent seen for ruthenium, as evidenced by the presence of metallic iridium at low iridium coverage. STEM imaging revealed a similar growth behavior for both iridium and ruthenium, starting from small clusters at low loadings to an interconnected network of crystalline nanoparticles at higher loadings.

The existence of Ru–O–C bonds could indicate to the root cause of the improved Ru OER catalyst stability on Pt–NSTF: the strong bonding of Ru to Perylene Red could increase the surface area of the deposited OER nanoparticles by preventing coalescence and reduce the rate of dissolution in an electrochemical environment. Thus, these findings revealed a fundamental relationship that provides a basis for understanding the electrochemical behavior of these materials.

*Acknowledgements*. This work was supported by the DOE Fuel Cell Technology Office, Award No. DE-EE0000456 and the Oak Ridge National Laboratory's Shared Research Equipment (ShaRE) User Program, sponsored by the Office of Basic Energy Sciences, U.S. DOE.

И З В О Д

## XPS И STEM ПРОУЧАВАЊЕ ФОРМИРАЊА МЕЂУСЛОЈА ИЗМЕЂУ УЛТРА-ТАНКОГ Ru И Ir КАТАЛИТИЧКОГ СЛОЈА ЗА РЕАКЦИЈУ ИЗДВАЈАЊА КИСЕОНИКА И ПОДЛОГЕ ОД ВИСКЕРА ПЕРИЛЕН-ЦРВЕНОГ

LJILJANA L. ATANASOSKA[1], DAVID A. CULLEN[2] и RADOSLAV T. ATANASOSKI[1]

*[1]3M Co., 3M Center, St. Paul, MN, 55144-1000 USA и [2]Materials Science and Technology Division, Oak Ridge National Laboratory, Oak Ridge TN 37831 USA*

(Received 27 September 2013)

Проучавано је формирање међуслоја између нано-структурних вискера перилен--црвеног (PR) и рутенијум и иридијум катализатора за реакцију издвајања кисеоника (OER) коришћењем XPS и STEM техника. Површински слојеви катализатора за OER дебљине ≈0,1 до ≈50 nm су *ex situ* депоновани из гасовите фазе на PR. STEM фотографије су показале да се, са повећањем дебљине, Ru и Ir трансформишу од аморфних кластера у кристалиничне нано-честице, са агломератима који превазилазе дебљине површинског слоја. XPS подаци показују јаку интеракцију између Ru и PR. Ir такође реагује са PR, мада не у степену регистрованом за Ru. При ниским степенима покривености целокупни Ru је прореаговао, док је мала количина Ir остала у металном облику. Ru и Ir се везују на PR карбонилним местима, што показује смањење фотоемисије са карбонилних места и преклапање нових пикова који се приписују једнострукој вези C–O. Анализа

фитоване криве и изведена стехиометрија указују на формирање метало–органских веза. Очигледно је и паралелно постојање оксидних веза.

(Примљено 27. септембра 2013)

REFERENCES

1. R. T. Atanasoski, L. L. Atanasoska, D. A. Cullen, G. M. Haugen, K. L. More, G. D. Vernstrom, *Electrocatalysis* **3** (2012) 284
2. M. Shao, *Electrocatalysis in Fuel Cells: A Non and Low Platinum Approach,* Springer, New York, 2013, p. 637
3. R. T. Atanasoski, D. A. Cullen, G. D. Vernstrom, G. M. Haugen, L. L. Atanasoska, *ECS Electrochem. Lett.* **2** (2013) F25
4. 2010 DOE Hydrogen Program Review, http://www.hydrogen.energy.gov/pdfs/ review10/ /fc006_atanasoski_2010_o_web.pdf (accessed in September 2013)
5. D. A. Cullen, K. L. More, K. S. Reeves, G. D. Vernstrom, L. L. Atanasoska, G. M. Haugen, R. T. Atanasoski, *ECS Trans.* **41** (2011) 1099
6. L. L. Atanasoska, D. A. Cullen, A. Hester, R. T. Atanasoski, *ECS Trans.* **50** (2013) 19
7. L. Atanasoska, W. O'Grady, R. Atanasoski, F. Pollak, *Surface Sci.* **202** (1988) 192
8. L. Atanasoska, S. Anderson, H. M. Meyer III, Z. Lin, J. H. Weaver, *J. Vac. Sci. Technol., A* **5** (1987) 3325
9. L. Atanasoska, H. M. Meyer III, S. Anderson, J. H. Weaver, *J. Vac. Sci. Technol*., *A* **6** (1988) 2175
10. L. Atanasoska, R. Atanasoski, S. Trasatti, *Vacuum* **40** (1990) 91.